Sigma J Eng Nat Sci, Vol. 43, No. 6, pp. 2006−2016, December, 2025

Sigma Journal of Engineering and Natural Sciences
Web page info: https://sigma.yildiz.edu.tr
DOI: 10.14744/sigma.2025.1930

Research Article

Ultrasonic waveguide sensor design using bend reflectors for elastic moduli and temperature measurement

Anubhav SRIVASTAVA[1,*], Arun VALABHOJU[1], Abhishek KUMAR[1], Suresh PERIYANNAN[1,*]

[1]*Department of Mechanical Engineering, National Institute of Technology, Warangal, 506004, India*

ARTICLE INFO

Article history
Received: 08 May 2024
Revised: 21 August 2024
Accepted: 17 October 2024

Keywords:
Elastic Moduli; Sensors; Temperature; Time of Flight; Ultrasonic Strip Waveguide

ABSTRACT

This research presents an ultrasonic strip waveguide sensor with various reflector embodiments, including rectangular notches, single, and multiple bends. The ultrasonic waveguide sensor concept is a non-destructive and non-invasive method to measure material properties in elevated temperatures, where conventional techniques often fail. This ultrasonic sensor technique measures the surrounding temperature of the waveguide and its temperature-dependent elastic moduli using the symmetric (S_0) wave mode. Initially, we performed the Finite Element Method (FEM) simulations using Abaqus CAE software to find a better ultrasonic reflector configuration and its dimension based on the ultrasonic waveguide (S_0 mode) signal behavior. The simulation uses a rectangular strip waveguide (stainless steel) with a thickness of 0.5 mm, a width of 3 mm, and a length of 1000 mm. The S_0 mode was excited using a Hanning pulse tone burst signal at one end of the waveguide. Then, FEM studies revealed that the reconfigurable bend reflector (radius 3 mm) is better than rectangular reflector configurations for designing the ultrasonic sensor to obtain better reference reflection. Then, ultrasonic-guided wave experiments were conducted at different temperatures using the same dimension of the stainless-steel strip as a waveguide using the pulse-echo approach with an ultrasonic shear transducer at one end of the waveguide. We considered the ultrasonic parameter time of flight difference to calibrate the sensor based on the surrounding temperature. Also, temperature-dependent elastic moduli were measured, resulting in a maximum measurement error of 3% compared to literature data. The developed novel waveguide technique comprising non-destructive method can easily measure the elastic moduli compared to conventional destructive type testing methods, specimens are reusable, monitoring the components in service, and simple and cost-effective technique for monitoring various industrial components like power plants, oil, and Petro-chemical industries.

Cite this article as: Srivastava A, Valabhoju A, Kumar A, Periyannan S. Ultrasonic waveguide sensor design using bend reflectors for elastic moduli and temperature measurement. Sigma J Eng Nat Sci 2025;43(6):2006−2016.

***Corresponding author.**
*E-mail address: as22mem4r03@student.nitw.ac.in, sureshp@nitw.ac.in

This paper was recommended for publication in revised form by Editor-in-Chief Ahmet Selim Dalkilic

Published by Yıldız Technical University Press, İstanbul, Turkey

INTRODUCTION

Ultrasonic testing is a well-known nondestructive testing (NDT) technique that utilizes high-frequency sound waves. In ultrasonic testing, the ultrasonic waveguide technique can be used for various applications, such as measurements of the temperature of the surrounding medium, liquid level, rheological properties of fluids, and material properties. In hostile environments, conventional sensors like thermocouples, RTDs, etc., show accuracy problems, whereas ultrasonic sensors can work efficiently. Significant work has been done on ultrasonic sensors in the past few years. Balasubramanium et al. classified the ultrasonic waveguide sensing technique into two broad categories, the forward problem and inverse problem, implying its applications in process industries [1]. Periyannan et al. [2] reported a novel ultrasonic technique for determining elastic moduli (E) using cylindrical waveguides at different temperatures. Bao et al. [3] developed a new sonic resonance method to measure Young's modulus (E) and shear modulus (G) of rail steel at elevated temperatures. They used a laser vibrometer to observe the flexural and torsional resonance frequency at elevated temperatures and used it to measure E and G, respectively. N. Raja et al. demonstrated using a stainless-steel (SS) rod-like waveguide for distributed skin temperature measurement in solid pipes and water. They used bend-notch and notch-notch combinations as sensor regions co-located with the K-type thermocouples for calibration. [4]. Periyannan et al. reported a robust technique for multi-level temperature measurements using six Chromel waveguides of diameter 1.12 mm with varying lengths attached to a single shear transducer for transmitting and receiving the ultrasonic signals. The difference in time in flight and readings from co-located K-type thermocouples were used to calibrate the sensor [5]. Liao et al. have extended the ultrasonic dry-coupled waveguide technique in structural health monitoring (SHM) of critical mechanical components in high-temperature environments [6].

Zhou et al. [7] proposed a high-accuracy ultrasonic temperature estimation technique. They employed maximum length sequence (MLS) modulation on a continuous wave to effectively suppress the effects of echoes. The temperature of distilled water was successfully measured with an error of ±0.04^{0}C. Periyannan et al. [8] developed a novel technique to measure the temperatures at multiple locations using multiple waveguides with a single bend and a single waveguide with multiple bends. Sahu et al. [9] reported the use of an ultrasound-guided wave technique for mapping the surface temperature of Aluminum plates. A metal strip with rectangular notches was placed in the slots of two Aluminum plates. Shear horizontal (SH_0) wave mode was excited in the waveguide with the help of an ultrasonic shear transducer attached at one end of the waveguide. The waveguide sensor was calibrated using reference temperatures obtained from the data of co-located RTDs. Szelek et al. [10] presented a new evaluation method for temperature-dependent ultrasonic longitudinal and shear velocity measurements. The results obtained from these ultrasonic velocities were further used to determine elastic and shear moduli E and G, respectively. Liang et al. [11] reported a sapphire ultrasonic temperature sensor for monitoring the temperature of an aircraft engine. Periyannan and Balasubramaniam reported a novel technique for the measurement of temperature and temperature-dependent elastic moduli (E(T) and G(T)) using straight and L-bend waveguides with L (0, 1) and T (0, 1) wave modes generated using pulse-echo mode through longitudinal and shear wave transducers, respectively. [12]. Dhayalan et al. developed a novel non-invasive ultrasonic waveguide sensor for liquid level measurement. [13]. Periyannan et al. reported a novel re-configurable ultrasonic temperature sensing technique using a helical spring-like waveguide with multiple notches as reflector embodiments [14].

Nishanth et al. [15] introduced an ultrasonic waveguide technique for distributed temperature measurement on a solid surface. A stainless-steel bent rod waveguide of 1 mm diameter with axisymmetric notches in the bent horizontal region acts as the sensor. Changes in the time of flight of the waves, reflected from the bend and notches, were estimated and used for calibration with the results of K-type thermocouples co-located in the sensor region. Wong et al. [16] presented a precise method for measuring temperatures up to 200°C using ultrasonic waves. Wang et al. [17] proposed a novel U-shaped waveguide sensor for viscosity measurement using a pitch-catch method to excite and receive an SH_0 wave. Kumar et al. [18] demonstrated an ultrasonic waveguide sensor for fluid level sensing using a U-shaped and helical waveguide. They also reported minute-level sensing using flexural wave mode [19, 20]. Balasubramaniam and Periyannan developed an ultrasonic waveguide technique to measure the surrounding media's chemical and physical properties [21, 22]. Signal processing is a significant step in the development of an accurate sensing device; extensive studies of various signal behaviors and analytical solutions are discussed in the literature and used in signal processing in various sensors' sensing applications [23-35]. Uses of NDT techniques are not limited to only metallic materials. Gezer et al. used NDT methods to detect defects in a wooden structure [36]. And Kabay et al. utilized the NDT technique to estimate the core compressive strength of concrete.[37].

Earlier research on ultrasonic waveguide sensors predominantly focused on cylindrical waveguides, emphasizing line contact with the transducer surface. Due to line contact, it may not effectively transmit the ultrasonic energy in the waveguide [2, 8, 14, 21, 22]. However, strip waveguides offer enhanced surface contact with the transducer for transmitting the ultrasonic energy effectively in the waveguide due to surface contact. The early works reported ultrasonic reflector dimension (bend radius = 3d (d - wire diameter)) and their empirical constant A=2.5 for E measurements of the cylindrical specimens using L(0, 1) wave mode [38, 39]. However, these are not reported for strip waveguides in the case of strip specimens' E measurements. The wave propagation behavior may differ in strip specimens (rectangular cross-section) compared to cylindrical specimens due to different geometry/boundaries. Hence, this work reported that E measurements of the strip specimens, ultrasonic reflector dimension (bend radius = 6t (t - strip thickness)), and their empirical constant (A=2) were found using S_0 wave mode. In engineering applications, plenty of metal/alloy strips or bars are generally used.

Furthermore, there is a lack of research on using strip waveguides for Young's modulus (E) estimation as a function of temperature. Hence, this study uses the novel concept to investigate the potential of strip waveguides for temperature-dependent elastic moduli (Ei) measurements [21, 22]. Further, it can act as an ultrasonic temperature sensor too [40, 41].

FINITE ELEMENT METHOD SIMULATIONS

Finite element method (FEM) simulations for the waveguide with different reflector embodiments were conducted using Abaqus software. The material properties and FEM parameters used in the simulation, as shown in Table 1. Initially, wave propagation characteristics in the waveguide were studied using the Disperse calculator/software based on waveguide thickness (0.5 mm). The non-dispersive guided wave propagation velocity and its corresponding frequencies were identified (Fig.1a) [42].

Then, the S_0 wave mode in the waveguide was observed to be non-dispersive in the 200-500 kHz frequency range and then, followed a well-known concept to verify the operating frequency and non-dispersive group velocity using a FEM study and its parameters (2D FFT Vs wave number) [9, 39, 41]. The S_0 wave mode (red line) was ensured to pass through a 200-360 kHz frequency spectrum region. This study was conducted in the frequency bandwidth of 250-350 kHz within the non-dispersive region. We obtained a 2D FFT plot (Fig. 1b) based on received signals from FEM simulations, and these simulations were compared with a dispersion plot.

Table 1. Material properties of SS304 and FEM parameters used in the simulation

Material properties	FEM parameters
Material – SS304	Solver – Abaqus CAE
Density – 7960 kg/m^3	Module – Dynamic, explicit
Young's modulus – 195 GPa	Time increment (t) – 1e^{-8}
Poisson's ratio – 0.27	Element type – C3D8R
	Element size – 0.25 mm
	Frequency (f) – 0.250 MHz
	No. of cycles (n) – 3

Waveguide Sensor Design with Destructive and Non-destructive Type Reflectors

Different reflector embodiments like rectangular notch, single bend, and multiple bends were introduced in the strip waveguides using the Abaqus CAE software, as shown in Figure 2**,** with respective dimensions. Ultrasonic waves were reflected from these reflector embodiments while propagating through the waveguide. The waveguide sensor was designed with a single rectangular notch (made through waveguide thickness) by removing the material to create an ultrasonic (destructive type) reflector, as shown in Figure 2b. The destructive type reflector is useful in case the waveguide material is brittle. The depth of the rectangular notch used was through-thickness (0.5 mm) based on earlier reported literature [4, 21, 22]. The bend configurations (single bend and multiple bends) were preferred over the rectangular notch to make a non-destructive type reflector in the waveguide, as shown in Figure 2c and d. Bend reflectors were more suitable, easy to make, and re-configurable while designing the waveguide sensor using ductile materials. The bend acts as a better reference signal reflector for making an ultrasonic temperature sensor without a temperature gradient, as reported by Periyannan [8]. While using a notch reflector, the waveguide sensors couldn't be

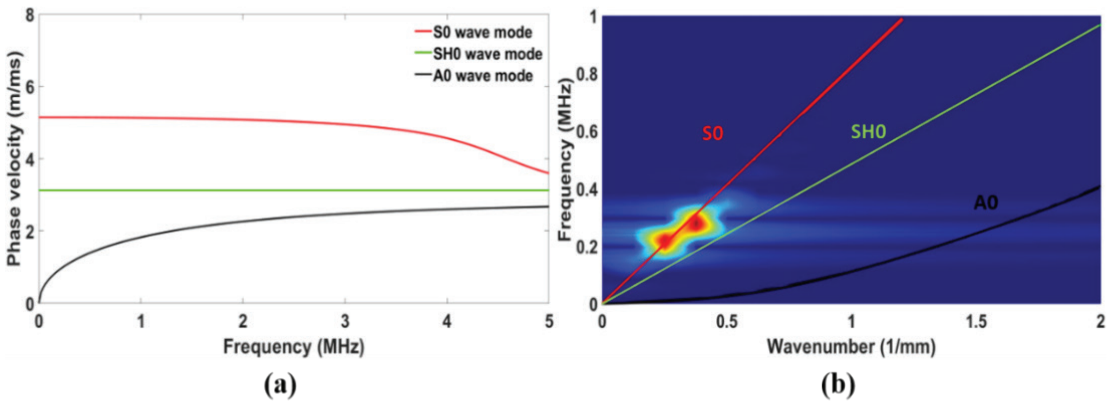

Figure 1. (a) Frequency vs. Phase velocity plot from Dispersion calculator (b) 2D FFT plot.

re-configured, as we wouldn't obtain the waveguide's original geometry. Single-bend waveguides could be useful for single-location measurements, and multiple-bend waveguides could be useful for multi-location measurements. The strength of the ultrasonic reflected signals from the bend reflector could be tuned/varied based on requirements by varying the bend radii. Hence, studies were carried out to determine suitable bend radii for designing the waveguide with distributed bend reflectors, as shown in Table 2, through case A to case D, by varying the radii from 4.5 mm to 10.5 mm for bends.

Stress wave propagation FEM simulations with S_0 wave mode were performed using Abaqus CAE software. A 3-cycle 250 kHz Hanning pulse signal (input excitation) was applied at one end of the waveguide in the FEM simulations, as shown in Eqn. (1). The A-scan (wave propagation time vs. displacement amplitude) plots for all the waveguides (Fig. 2b-d) were obtained, as shown in Figure 3 a-c. The bend reflectors' dimensions were optimized by studying the ultrasonic wave reflections (analyzed using the Hilbert transform tool, Fig. 4) at different bend radii of strip waveguide (Fig. 2 d) using the FEM approach in four Cases (A-D), as shown in Table 2, based on early reported work by Periyannan [8]. Nearly uniform amplitude reflections were obtained from each bend reflector for Case C, as shown in the Hilbert Transform in Figure 4. However, a uniform reflected signal strength was appropriate for making multiple bent sensors [8]. Hence, Case C was found to be a more suitable bend reflector configuration based on results obtained using the FEM approach, as shown in Figure 3c. Then, studies were carried out for the single-bend reflector in the waveguide while varying bend radii from 3 mm to 12 mm, as shown in Figure 3b. Then, it was observed that as the radius decreased, the amplitude of the reflected signal increased, nearly equal to the end reflection for a 3 mm radius. Hence, a 3 mm bend radius was found to be more suitable. Similarly, it was observed that the amplitude of the reference reflected signal increased from the rectangular notch reflector (destructive type) while increasing the width of the notch from 0.3 mm to 1 mm, as shown in Figure 3a. Here, the strength of the reflected signals from the notch and waveguide end was nearly the same when the width of the notch was 1mm.

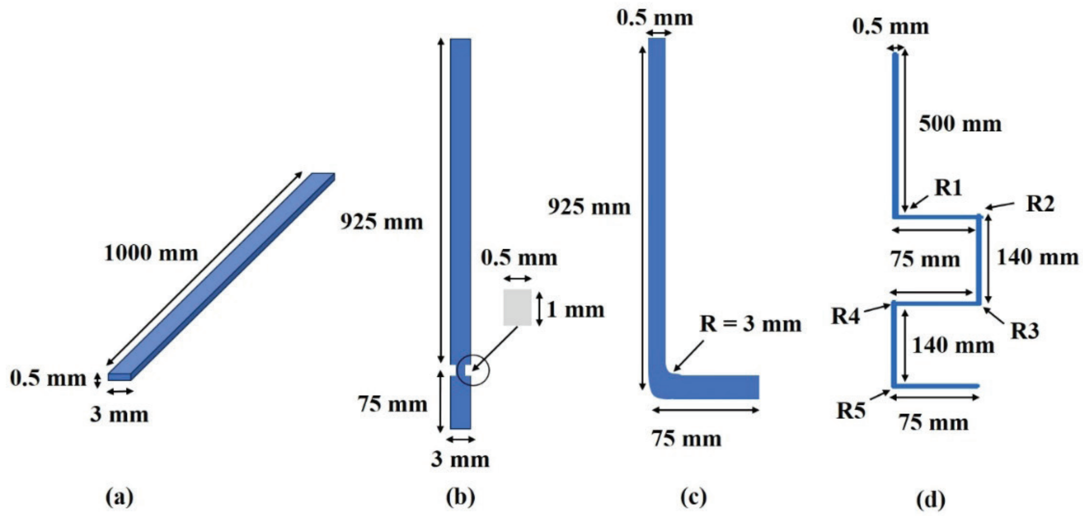

Figure 2. Waveguides with (a) no reflector, (b) rectangular notches through the thickness, (c) single bend, and (d) multiple bends.

Table 2. Bend radii in different cases

Cases	R1	R2	R3	R4	R5
Case A	1.5w	1.75w	2.0w	2.25w	2.5w
Case B	2.5w	2.25w	2.0w	1.75w	1.5w
Case C	3.0w	2.75w	2.5w	2.25w	2.0w
Case D	3.5w	3.25w	3.0w	2.75w	2.5w

All dimensions in mm. Note: width of the waveguide (w) = 3 mm.

$$H = [1 - cos\left(\frac{2\pi f t}{n}\right)].cos(2\pi f t) \quad (1)$$

Different ultrasonic reflectors (Fig. 2) were studied using the FEM approach to find a suitable ultrasonic reflector. It was observed that bend embodiments (non-destructive reflectors) were appropriate ultrasonic reflectors due to their reconfigurability and ability to tune the reflector's signal strength based on our requirements, as shown in Figure 3b and c. However, a single-bend reflector was initially preferred when designing the ultrasonic sensor to measure the waveguide materials' temperature and elastic moduli.

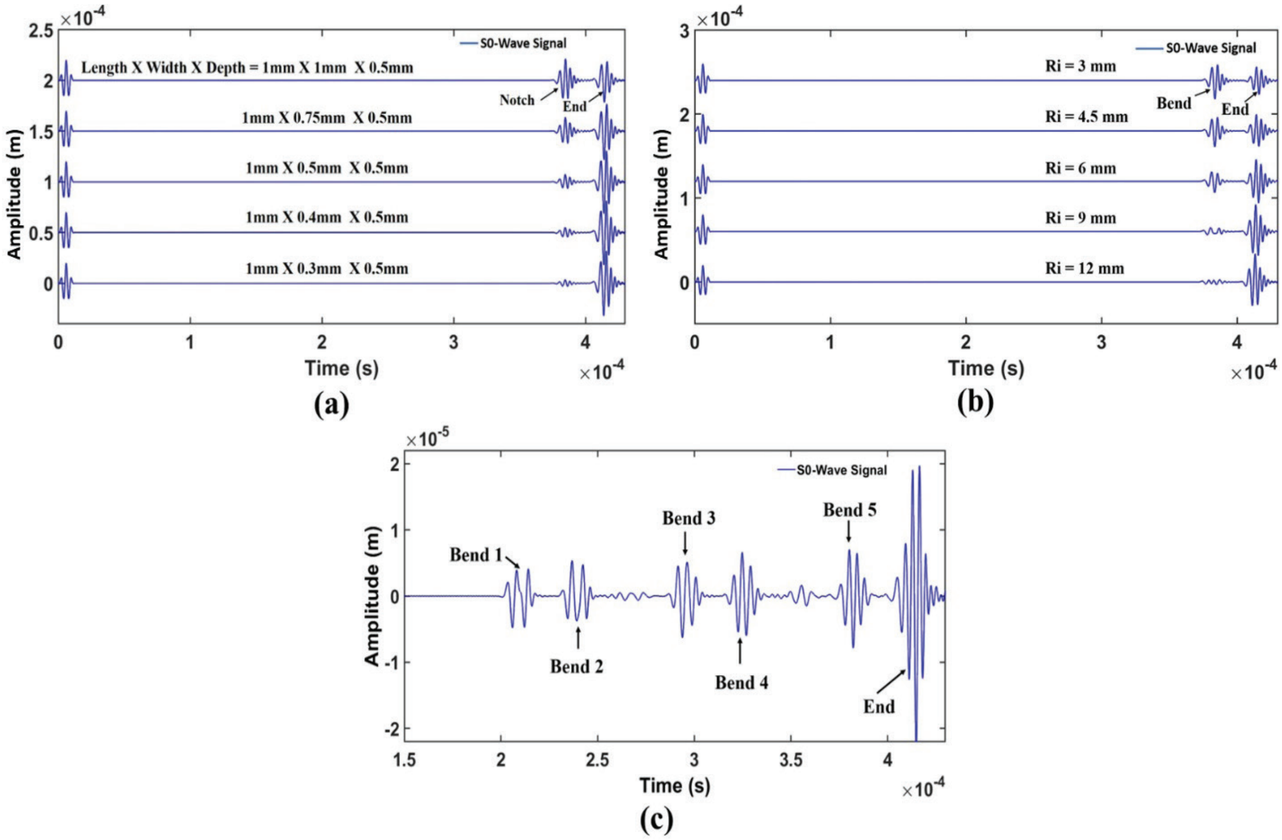

Figure 3. A-Scans of S_0 wave for a waveguide with (a) rectangular notch (b) single bend, and (c) multiple bends.

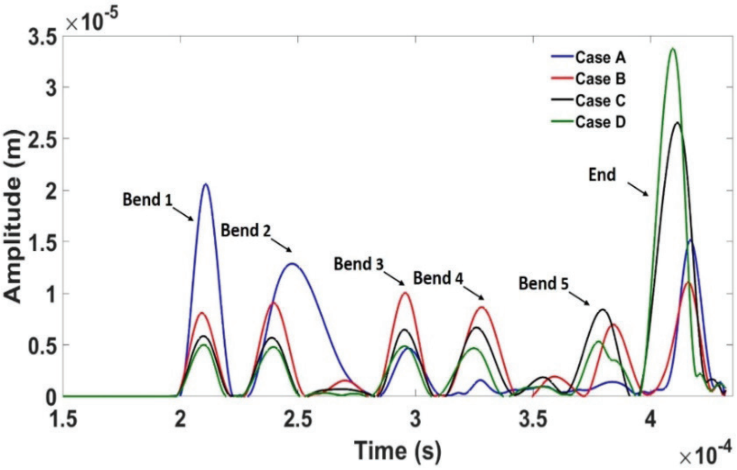

Figure 4. Hilbert transforms different cases to determine suitable bend radii.

EXPERIMENTAL METHODOLOGY

At elevated temperatures, the properties of metals/alloys show significant variation. Periyannan et al. reported the variation of elastic moduli at elevated temperatures of various metals/alloys [2]. Using cylindrical waveguides, they estimated the temperature-dependent Young's and Shear modulus of Inconel-690, Copper, Aluminum, Kanthal, etc. Simmons and Van Echo had well-documented elastic moduli of various types of stainless steel [40]. This research work was intended to develop an ultrasonic strip waveguide sensor that could be utilized to estimate temperature-dependent Young's modulus. Here, a rectangular cross-section (strip) waveguide was used, which provides better surface contact with the transducer surface than cylindrical waveguides. FEM simulation studies on various reflector embodiments suggested that bend reflectors with appropriate bend radii were more suitable based on the reflected signal's amplitudes of A-scan plots, as shown in Figure 3 and Figure 4. The strip waveguide (with bend) approach was followed for estimating the temperature and temperature-dependent Young's modulus of waveguide material. An SS304 strip waveguide with an L-bend (which acts as a sensor region) was used for experiments. The straight portion of the waveguide was 925 mm, and the bend portion was 75 mm long. The technique is illustrated in Figure 5 through a schematic diagram of the experimental setup, where we can see the strip waveguide coupled to the shear transducer (Olympus, V151, 500 kHz, 1-inch diameter, USA) at an angle of 0° to excite the S_0 wave mode and the shear transducer further connected to a personal computer and analog to digital converter as well as to record the data using Pico-Scope. Using silicone grease couplant at one end of the waveguide avoids air gaps between the transducer and the waveguide. We used a pulse-echo approach to transmit and receive S_0 wave mode in the waveguide using JSR Ultrasonic DPR 300 and Pico Scope 3000 series, respectively. During the experiments, control parameters were input voltage 475 V, gain 36 dB, bandpass filter 0-7.5 MHz, pulse-echo frequency 250 kHz, and 100 MHz sampling rate.

The waveguide was exposed inside the temperature-controlled furnace with the L-bend as a measurement point. A thermocouple was co-located with the sensor region to record temperature data at uniform intervals. The transducer was fixed outside the furnace to avoid damage due to high temperature. A bend radius of 3 mm was found to be better for a single-bend sensor design (L-bend) from the FEM simulation study using different bend radii, as shown in Figure 6a. Rose documented the ultrasonic S_0 wave propagation in waveguides [38]. And S_0 velocity was ensured under the non-dispersive region with the help of the Dispersion calculator [42]. Experiments were carried out at room temperature with different bend radii. The results of the simulation studies and experiments were in good agreement, as depicted in the A-scan signals (Fig. 6a-b). Here, the ultrasonic reflection was reduced from the bend while the bend radius was increased, and simultaneously, the end reflection was increased. If the bend radius decreased, then ultrasonic reflection from the bend was increased, and end reflection was decreased, which can be observed from FEM studies and experimental studies, as shown in Figure 6c-d, and finally, observed that a bend radius of 3 mm to 4.2 mm was appropriate to make an optimum bent reflector. Air was the surrounding medium in the furnace, whose physical properties were known a priori. The ultrasonic parameter's difference in time of flight (δToF) was used to calibrate the sensor. We evaluated the δToF by a peak tracking algorithm on reflected signals obtained from the bend and end of the waveguide at different temperatures, as reported by Periyannan [2].

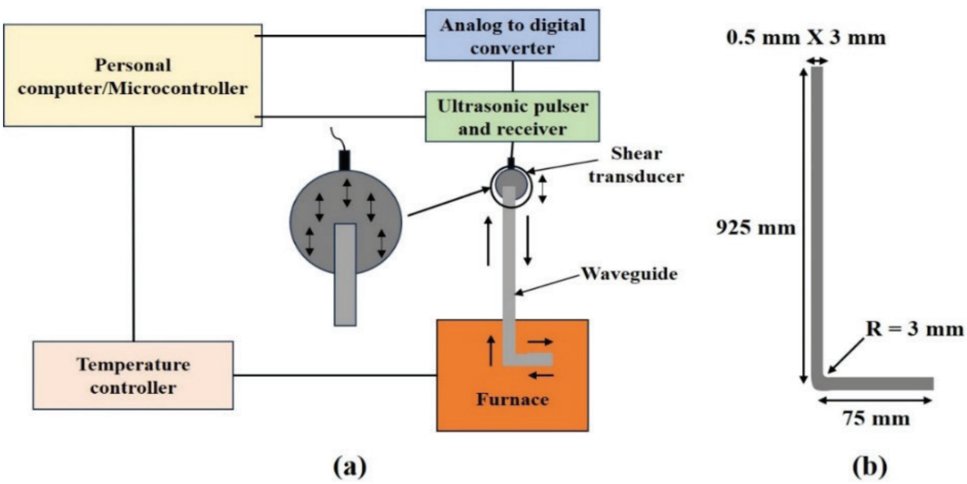

Figure 5. (a) Schematic diagram of the experimental setup, (b) bent waveguide.

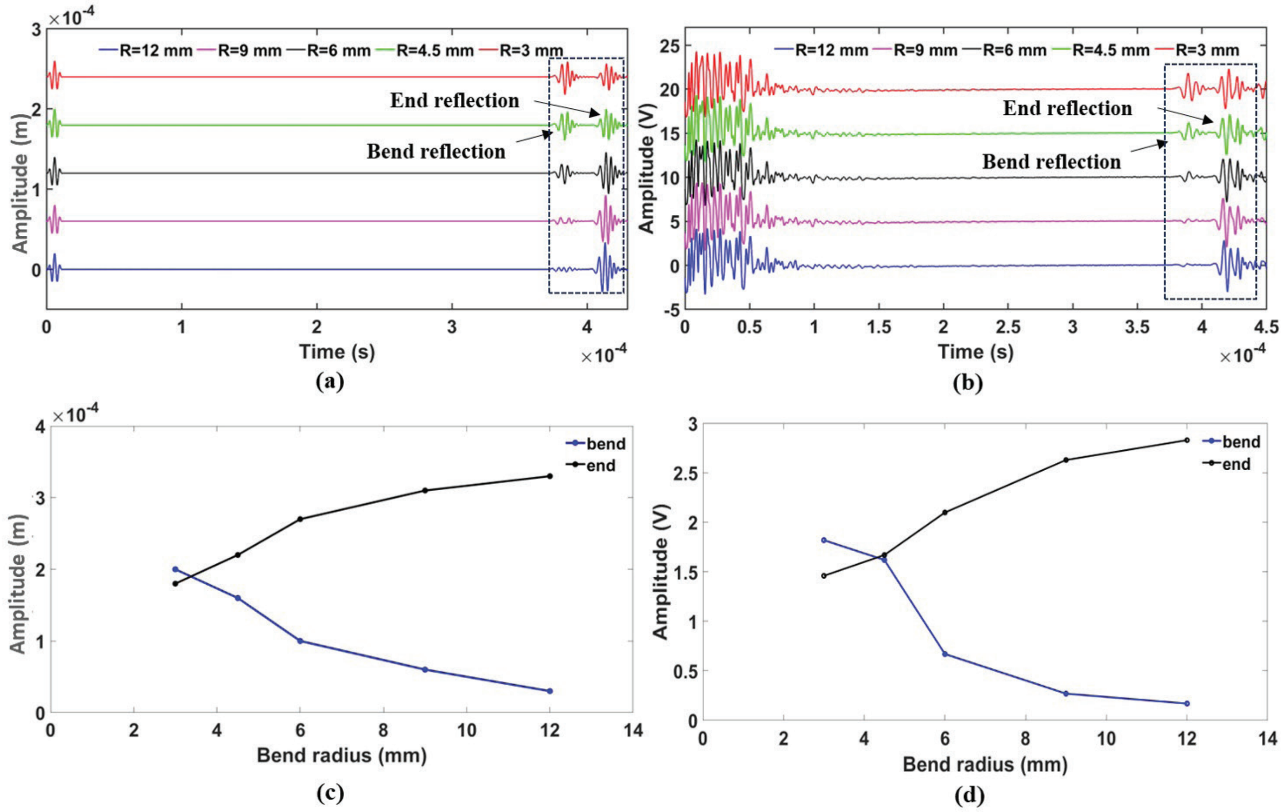

Figure 6. (a) Simulation A-scans, (b) experimental A-scans, (c) simulation amplitude decay with bend radii, and (d) experimental amplitude decay with bend radii.

RESULTS AND DISCUSSION

Experiments were performed in a range of temperatures from 30 °C to 630 °C using a furnace. At an interval of every 10 °C, A-scan signals were obtained at different temperatures due to S_0 wave mode reflection from the bend and end of the waveguide. A clear time/phase shift was observed in A-scan plots due to the changing behaviors of ultrasonic waves at different surrounding temperatures and thermal expansion of waveguide material, as shown in Figure 7, reflected signals shifting towards the right with the increase in temperature from 30°C to 600°C. A peak tracking algorithm was employed to estimate δToF using equations (2) and (3).

$$ToF_o = (ToF_e - ToF_b) \tag{2}$$

$$\delta ToF_i = [(ToF_{ei} - ToF_{bi}) - (ToF_e - ToF_b)] \tag{3}$$

Where, $ToF_{e,b}$ – Time of flight from end (e) and bend (b) at room temperature

$ToF_{ei,bi}$ – Time of flight from the end (e) and bend (b) at the instantaneous temperature

ToF_o – Difference in time of flight from the end and bend at room temperature

δToF_i – Difference in time of flight at instantaneous temperature.

A thermocouple was co-located near the bend region to collect the temperature data throughout the experiment. The ultrasonic sensor was calibrated using the δToF and thermocouple data at various time instants. The co-located thermocouple and waveguide sensor's δToF measurements were used to calibrate the sensor for surrounding temperature measurement. We conducted multiple experiments, and the data from all three experiments were in close agreement, ensuring repeatability evident from the calibration curves of all three experiments, as shown in Figure 8 (a).

Periyannan measured Young's modulus (E) of cylindrical waveguide materials based on L (0,1) wave mode at various temperatures and reported the empirical constant "A=2.5" suitable for cylindrical waveguides. [2]. In this work, the Ei of a strip waveguide was measured using equation (4) based on the S_0 wave mode. The empirical constant fund A =2 for the strip-like waveguide material while comparing (Ei vs Ti) with the literature.

$$Ei = \left(\frac{Eo}{1 + A\left(\frac{\delta ToFi}{ToF}\right)} \right) \quad (4)$$

Here, *Ei* - Young's modulus at instantaneous temperature *Eo* - Young's modulus at room temperature (195 GPa).

The sensor was calibrated based on temperature-dependent E measurement using ToF and δToF data in equation (3). The calibration curve is shown in Figure 8b.

Equation (5) denotes the calibration equation for temperature sensing, where "y" denotes temperature and "x" denotes δToF. Equation (6) denotes the calibration equation for temperature-dependent Young's modulus estimation for the waveguide material (SS304) using an ultrasonic strip waveguide sensor, where "y" denotes Young's modulus and "x" denotes temperature. The error was calculated using equation (7). *Ei* computed using equation (4) was compared to the *Ei* given in literature data [40].

$$y = -12.92x^2 + 185.02x + 42.18 \quad (5)$$

$$y = -2.00e^{-5}x^2 - 0.061x + 197.10 \quad (6)$$

$$\%\,Error = \frac{|Ultrasonic\ sensor\ data - Literature\ data|}{Literature\ data} X\,100 \quad (7)$$

Table 3 shows the % error in measuring Ei at various temperatures using a strip waveguide sensor compared to the literature data from ASTM [40]. The results were compared to the recent technique and available ASTM literature [2, 40]. The maximum error observed using a strip waveguide was 3 %, whereas the maximum error for the cylindrical waveguide sensor was 6.2 % [2]. Strip waveguide

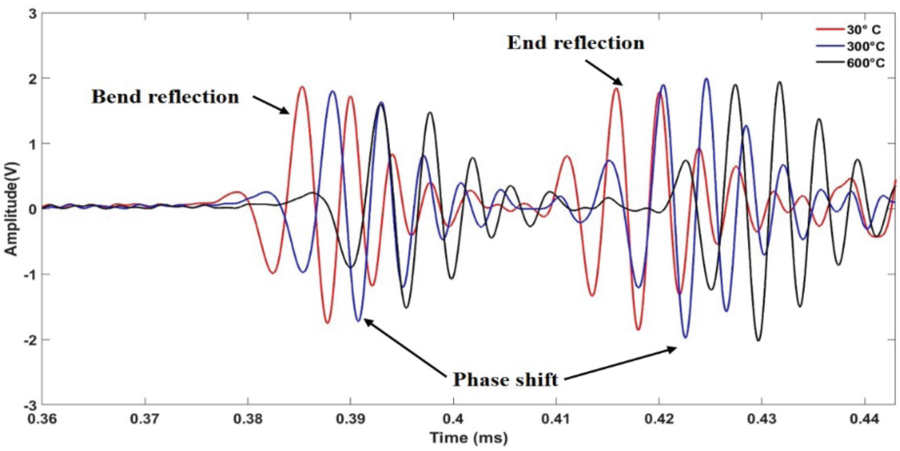

Figure 7. Phase and time shifted A-scan signals at 30°C, 300°C, and 600°C.

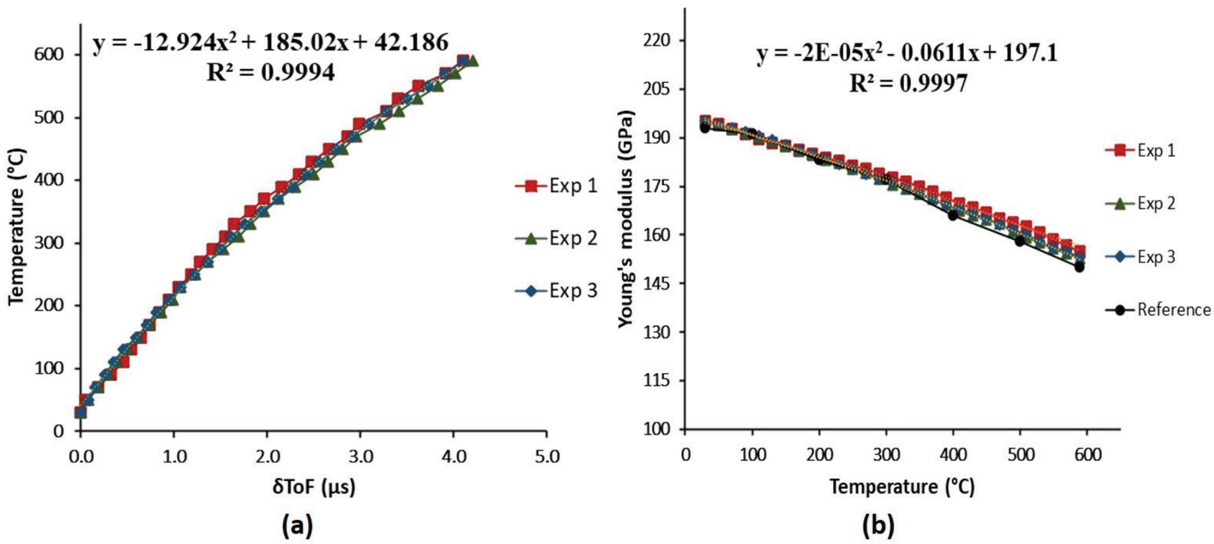

Figure 8. Calibration curves (a) δToF vs. Temperature, and (b) Temperature vs. Young's modulus.

Table 3. Error in the measurement of Ei calculated using strip waveguide sensor and cylindrical waveguide sensor

Temperature (°C)	Literature data Ei (GPa)	Ultrasonic strip waveguide sensor data Ei (GPa)	% Error for strip waveguide sensor	Ultrasonic cylindrical waveguide sensor data Ei (GPa)	% Error for cylindrical waveguide sensor
30	193	195	1.0	205	6.2
100	191	190.94	0.03	197.4	3.3
200	183	184.12	0.65	186.2	1.7
300	177	176.9	0.05	175.8	0.6
400	166	169	2.0	168	1.2
500	156	161.2	3.0	159.3	2.1
600	150	152.8	1.86	147	2.0

sensors' lower and upper error limits were 0.03 % and 3 %, respectively. Also, the observed error difference in both techniques may be due to experimental settings, the type of material/compositions, the initial E_0 values, and their geometries [43].

Since bend reflectors are non-destructive, material removal (notches) is not required to make ultrasonic reflectors. Hence, the waveguide is not permanently damaged but is reconfigurable and reusable. The intensity of the reflected signals can be tuned by varying the bend radius for sensor design. Especially using long waveguides with more bends for distributed temperature sensing. The effect of temperature gradient can be negligible in the horizontal bend region, which can be a better sensor [8].

CONCLUSION

We developed an ultrasonic strip waveguide sensor based on a symmetric wave mode to measure the elastic modulus and the surrounding medium temperature. The notch and bent reflectors were studied using the SS304 strip waveguide using the finite element method approach. The different bend radii were simulated using the finite element method approach to obtain a suitable bend radius and were compared to experimental studies. The bend radius of 3 mm was more appropriate, corresponding to the waveguide thickness for obtaining better signal reflection from the bend reflector. A thermocouple was placed in the bend region to monitor the temperature data at various intervals. We calibrated the sensor based on thermocouple data and the flight time difference. Then, the ultrasonic sensor's difference in time of flight and time of flight data were used to measure the temperature-dependent elastic modulus of the waveguide material at different temperatures. An empirical equation was obtained for the sensor by measuring the temperature-dependent elastic modulus at various temperatures. The measured Ei was compared to the available literature data and recent techniques; it was found to be in good agreement, and the error was ≤ 3 %. Multiple experiments were conducted to develop the ultrasonic temperature sensor and the E measurement as a function of temperature. The empirical constant "A=2" was found for strip waveguide material, and it was appropriate for evaluating the measure of the temperature-dependent elastic modulus of the material. Also, the sensor's repeatability was observed from multiple trials.

The ultrasonic sensors are more suitable in highly flammable or hazardous regions, such as furnaces for steel and glass melting industries. The stiffness of high-temperature materials/metals can be measured using this ultrasonic strip waveguide sensor concept for high-temperature industrial applications. A waveguide with multiple bend reflectors can also measure the hot chamber's distributed temperature. The further scope of ultrasonic waveguide sensors using bend reflectors includes optimizing bend designs and exploring advanced materials to enhance sensor performance at high temperatures. Multiple thermocouple measurements can be done using a single wire (any solid/elastic medium) acting as a waveguide with the distributed sensors: a simple concept and cost-effective technique for measuring multiple parameters simultaneously. Also, the ultrasonic sensor has no junction that can fail. This sensor concept can be extended to real-time monitoring systems for structural health, temperature sensing in power plants and oil industry pipelines, and non-destructive testing for monitoring various industrial components. Efforts toward commercialization and scalability will make this technology more accessible and impactful across diverse fields in industrial applications.

AUTHORSHIP CONTRIBUTIONS

Authors equally contributed to this work.

DATA AVAILABILITY STATEMENT

The authors confirm that the data that supports the findings of this study are available within the article. Raw data that support the finding of this study are available from the corresponding author, upon reasonable request.

CONFLICT OF INTEREST

The author declared no potential conflicts of interest with respect to the research, authorship, and/or publication of this article.

ETHICS

There are no ethical issues with the publication of this manuscript.

STATEMENT ON THE USE OF ARTIFICIAL INTELLIGENCE

Artificial intelligence was not used in the preparation of the article.

REFERENCES

[1] Balasubramaniam K, Raja N, Periyannan S. Ultrasonic waveguide sensors for measurements in process industries. In: IEEE Sensors. New Delhi, India: IEEE; 2018. p. 1-4. [CrossRef]

[2] Periyannan S, Balasubramaniam K. Moduli determination at different temperatures by an ultrasonic waveguide method. Exp Mech. 2016;56:1257-1270. [CrossRef]

[3] Bao Y, Zhang H, Ahmadi M, Karim MA, Felix WH. Measurements of Young's and shear moduli of rail steel at elevated temperatures. Ultrasonics 2014;54:867-873. [CrossRef]

[4] Raja N, Balasubramaniam K, Periyannan S. Ultrasonic waveguide-based multi-level temperature sensor for confined space measurements. IEEE Sens J 2018;18:5699-5706. [CrossRef]

[5] Periyannan S, Balasubramaniam K. Multi-level temperature measurements using ultrasonic waveguides. Meas 2015;61:185-191. [CrossRef]

[6] Liao Z, Zhang X, Liu T, Jia J, Tu ST. Characteristics of high-temperature equipment monitoring using dry-coupled ultrasonic waveguide transducers. Ultrasonics 2020;108:106236. [CrossRef]

[7] Zhou C, Wang Y, Qiao C, Zhao S, Huang Z. High-accuracy ultrasonic temperature measurement based on MLS-modulated continuous wave. Meas 2016;88:1-8. [CrossRef]

[8] Periyannan S, Rajagopal P, Balasubramaniam K. Ultrasonic bent waveguides approach for distributed temperature measurement. Ultrasonics 2017;74:211-220. [CrossRef]

[9] Sahu GP, Raja N, Balasubramaniam K. Surface temperature mapping of a metal plate using ultra-sound-guided wave technique. ASME J Nondestruct Eval 2021;4:041009. [CrossRef]

[10] Szelek J, Mackiewicz S, Gutkiewicz P. Ultrasonic measurement of the temperature dependence of elastic moduli in light alloys. Insight Nondestruct Test Cond Monit 2010;52:380-385. [CrossRef]

[11] Liang H, Yang F, Yang L, Liu Z, Wang G, Wei Y, Xue H. Research and implementation of a 1800°C sapphire ultrasonic thermometer. J Sens 2017;2017:9710763. [CrossRef]

[12] Periyannan S, Balasubramaniam K. Temperature gradients and materials properties measurements using ultrasonic guided waves. In: 11th European Conference on Non-Destructive Testing (ECNDT 2014). Prague, Czech Republic: ECNDT; 2014. p. 1-8.

[13] Dhayalan R, Saravanan S, Manivannan S, Rao BPC. Development of ultrasonic waveguide sensor for liquid level measurement in loop system. Electron Lett 2020;56:1120-1122. [CrossRef]

[14] Periyannan S, Rajagopal P, Balasubramaniam K. Re-configurable multi-level temperature sensing by ultrasonic "spring-like" helical waveguide. J Appl Phys 2016;119:1-8. [CrossRef]

[15] Nishanth R, Lingadurai K, Periyannan S, Balasubramaniam K. Ultrasonic waveguide-based distributed temperature measurement on a solid surface. Insight Nondestruct Test Cond Monit 2017;59:358-363. [CrossRef]

[16] Wong TY, Tang Y, Zou F, Su Z. An ultra-high accuracy temperature measurement method using acoustic waveguide. IEEE Sens J 2021;21:2618-2626.

[17] Wang G, Wang Q, Li F. A U-shape shear horizontal waveguide sensor for online monitoring of liquid viscosity. Sens Actuators A Phys 2018;284:35-41. [CrossRef]

[18] Kumar A, Periyannan S. Enhancing the ultrasonic waveguide sensor's fluid level sensitivity using through-transmission and pulse-echo techniques simultaneously. Rev Sci Instrum 2023;94:1-10. [CrossRef]

[19] Kumar A, Periyannan S. Helical waveguide sensor for fluid level sensing using L(0,1), T(0,1) and F(1,1) wave modes simultaneously. IEEE Sens J. Forthcoming. Manuscript Number: Sensors-61676-2023.

[20] Kumar A, Periyannan S. Experimental study of ultrasonic wave propagation in a long waveguide sensor for fluid-level sensing. Russ J Nondestruct Test 2024;60:132-143. [CrossRef]

[21] Balasubramaniam K, Periyannan S. Ultrasonic waveguide technique for distribute sensing and measurements of physical and chemical properties of surrounding media. US Patent 11,022,502. 2021.

[22] Balasubramaniam K, Periyannan S. Waveguide technique for the simultaneous measurement of temperature-dependent properties of materials. US Patent 10,794,870 B2. 2020.

[23] Jena BB, Mishra LN, Paikray SK, Misra UK. Approximation of signals by general matrix summability with effects of Gibbs phenomenon. Bol Soc Parana Mat 2020;38:141-158. [CrossRef]

[24] Mishra A, Padhy BP, Mishra LN, Misra U. On degree of approximation of signals in the generalized Zygmund class by using (E, r)(N, qn) mean. Kragujevac J Math 2023;47:131-141. [CrossRef]

[25] Bhat IA, Mishra LN. A comparative study of discretization techniques for augmented Urysohn type nonlinear functional Volterra integral equations and their convergence analysis. Appl Math Comput 2024;470:128555. [CrossRef]

[26] Bhat IA, Mishra LN, Mishra VN, Tunç C, Tunç O. Precision and efficiency of an interpolation approach to weakly singular integral equations. Int J Numer Methods Heat Fluid Flow 2024;34:1479-1499. [CrossRef]

[27] Karanjgaokar V, Rahatgaonkar S, Rathour L, Mishra LN, Mishra VN. Approximation of periodic functions by wavelet Fourier series. Int J Anal Appl 2024;22:61. [CrossRef]

[28] Paul SK, Mishra LN, Mishra VN, Baleanu D. Analysis of mixed type nonlinear Volterra-Fredholm integral equations involving the Erdélyi-Kober fractional operator. J King Saud Univ Sci 2023;35:102949. [CrossRef]

[29] Sharma MK, Bhargava AK, Kumar S, Rathour L, Mishra LN, Pandey S. A fermatean fuzzy ranking function in optimization of intuitionistic fuzzy transportation problems. Adv Math Models Appl 2022;7:191-204.

[30] Sharma MK, Dhiman N, Kumar S, Rathour L, Mishra VN. Neutrosophic Monte Carlo simulation approach for decision making in medical diagnostic process under uncertain environment. Int J Neutrosophic Sci 2023;22:8-16. [CrossRef]

[31] Rathour L, Singh V, Yadav H, Sharma MK, Mishra VN. A dual hesitant fuzzy set theoretic approach in fuzzy reliability analysis of a fuzzy system. Inf Sci Lett 2024;13:433-440. [CrossRef]

[32] Sharma MK, Chaudhary S, Rathour L, Mishra VN. Modified genetic algorithm with novel crossover and mutation operator in travelling salesman problem. Sigma J Eng Nat Sci 2024;42:1876-1883. [CrossRef]

[33] Negero NT, Duressa GF, Rathour L, Mishra VN. A novel fitted numerical scheme for singularly perturbed delay parabolic problems with two small parameters. Partial Differ Equ Appl Math 2023;8:100546. [CrossRef]

[34] Hogeme MS, Woldaregay MM, Rathour L, Mishra VN. A stable numerical method for singularly perturbed Fredholm integro-differential equation using exponentially fitted difference method. J Comput Appl Math 2024;441:115709. [CrossRef]

[35] Younus A, Dastgeer Z, Rathour L, Mishra LN, Mishra VN, Pandey S. Distinguishability criteria of conformable hybrid linear systems. Nonlinear Eng 2022;11:420-427. [CrossRef]

[36] Gezer ED, Selçuk BA. Determination of damage and defects in historical wooden structures using nondestructive test devices. Sigma J Eng Nat Sci 2020;11:127-134.

[37] Kabay N, Aköz F. Investigation of factors affecting core compressive strength and non-destructive testing of concrete. Sigma J Eng Nat Sci 2020;38:171-182.

[38] Rose JL. Ultrasonic waves in solid media. Cambridge, UK: Cambridge University Press; 1999.

[39] Periyannan S, Balasubramaniam K. Simultaneous moduli measurement of elastic materials at elevated temperatures using an ultrasonic waveguide method. Rev Sci Instrum 2015;86:1-8. [CrossRef]

[40] Simmons JH, Van Echo D. Report on elevated-temperature of stainless-steel properties. ASTM Data Ser Publ DS-5-S1. 1967.

[41] Raja N, Balasubramaniam K, Periyannan S. Ultrasonic waveguide based level measurement using flexural mode F(1,1) in addition to the fundamental modes. Rev Sci Instrum 2019;90:1-10. [CrossRef]

[42] Huber A. Dispersion calculator. Ultrasonics 2018.

[43] Smith M. ABAQUS/Standard user's manual (Version 6.9). Dassault Systèmes Simulia Corp; 2009.